Inflammation Is Necessary for Long-Term but Not Short-Term High-Fat Diet–Induced Insulin Resistance

Yun Sok Lee,[1,2,3] Pingping Li,[3] Jin Young Huh,[1,2] In Jae Hwang,[1,2] Min Lu,[3] Jong In Kim,[1,2] Mira Ham,[1,2] Saswata Talukdar,[3] Ai Chen,[3] Wendell J. Lu,[3] Guatam K. Bandyopadhyay,[3] Reto Schwendener,[4] Jerrold Olefsky,[3] and Jae Bum Kim[1,2,5]

OBJECTIVE—Tissue inflammation is a key factor underlying insulin resistance in established obesity. Several models of immunocompromised mice are protected from obesity-induced insulin resistance. However, it is unanswered whether inflammation triggers systemic insulin resistance or vice versa in obesity. The purpose of this study was to assess these questions.

RESEARCH DESIGN AND METHODS—We fed a high-fat diet (HFD) to wild-type mice and three different immuno-compromised mouse models (lymphocyte-deficient Rag1 knockout, macrophage-depleted, and hematopoietic cell-specific Jun NH_2-terminal kinase–deficient mice) and measured the time course of changes in macrophage content, inflammatory markers, and lipid accumulation in adipose tissue, liver, and skeletal muscle along with systemic insulin sensitivity.

RESULTS—In wild-type mice, body weight and adipose tissue mass, as well as insulin resistance, were clearly increased by 3 days of HFD. Concurrently, in the short-term HFD period inflammation was selectively elevated in adipose tissue. Interestingly, however, all three immuno-compromised mouse models were not protected from insulin resistance induced by the short-term HFD. On the other hand, lipid content was markedly increased in liver and skeletal muscle at day 3 of HFD.

CONCLUSIONS—These data suggest that the initial stage of HFD-induced insulin resistance is independent of inflammation, whereas the more chronic state of insulin resistance in established obesity is largely mediated by macrophage-induced proinflammatory actions. The early-onset insulin resistance during HFD feeding is more likely related to acute tissue lipid overload.
Diabetes **60:2474–2483, 2011**

Chronic tissue inflammation is an important cause of insulin resistance in obesity. A number of studies have demonstrated increased accumulation of adipose tissue macrophages (ATMs) in obese humans and rodents (1,2), and it is likely that macrophage-induced proinflammatory signaling is a key mediator of obesity-induced tissue inflammation. It has also been shown that a specific subpopulation of $CD11c^+$, M1-like macrophages account for the majority of the increased ATM content, and these macrophages secrete a variety of cytokines that cause decreased insulin sensitivity through both paracrine and endocrine mechanisms (3–5). A number of additional studies have shown that genetic deletion of macrophage inflammatory pathway components has a marked effect to protect against obesity-induced insulin resistance and glucose intolerance (6–8).

In addition to this inflammatory mechanism, it is also known that lipid overload can cause insulin resistance. Thus, acute administration of lipid infusions to humans and rodents rapidly causes decreased insulin sensitivity through mechanisms that still remain to be completely defined (9–11). In addition, insulin-resistant adipose tissue displays enhanced rates of lipolysis and the increased circulating free fatty acid (FFA) levels can cause decreased insulin sensitivity through a process called lipotoxicity (12). However, in obesity, the relative roles of inflammation and lipotoxicity as causes of insulin resistance remain to be fully defined.

Here, we have conducted detailed high-fat diet (HFD) time course studies in wild-type and immuno-compromised mouse models, such as macrophage- or lymphocyte-depleted mice, or hematopoietic cell-specific Jun NH_2-terminal kinase (JNK)–deficient mice, to assess whether inflammation triggers systemic insulin resistance or vice versa in obesity.

RESEARCH DESIGN AND METHODS

Animals and treatments. Seven-week-old male C57BL/6J mice were obtained from Daehan-Biolink (Korea) or The Jackson Laboratory and were housed in colony cages in 12-h light/12-h dark cycles. Rag1 knockout (KO) mice were purchased from The Jackson Laboratory. After a minimum 1-week stabilization period, mice (8 weeks old) were fed normal chow diet (NCD) until they were subjected to 60% HFD for the indicated time periods (Research Diets, Inc.). Thus, on the day of death, all of the HFD mice were compared with age-matched chow-fed mice. The average initial body weights in each group of mice were not different. For oral glucose tolerance test, the mice were fasted for 6 h and basal blood samples were taken, followed by oral glucose injection (1 g/kg). Blood samples were drawn at 10, 30, 60, 90, and 120 min after injection. Mouse clamp experiments were performed as described previously (13). Insulin-stimulated glucose disposal rate (ISGDR) was calculated as: ISGDR = glucose disposal rate (GDR; during the clamp) − basal GDR. Therefore, this value represents a measurement of the increase in GDR from the basal value (basal hepatic glucose production [HGP] = basal GDR = basal R_a) as a result of the insulin infused in the clamp. Because basal GDR is the same as basal HGP, the equation could also be ISGDR = GDR (during the clamp) − basal HGP. We calculated the total GDR during the clamp in the traditional way as glucose infusion rate (GIR) + HGP (during the clamp). During the clamps, insulin was infused at a constant rate of 8.0 mU/kg/min. For the clodronate experiments, liposome-encapsulated clodronate (100 mg/kg) was intraperitoneally injected into the mice 3 days before the onset of HFD (as a single injection), which was followed by the second and third injections every 3 days (14). Homeostasis model assessment of insulin resistance was calculated using the following formula: fasting glucose (mg/dL) × fasting insulin (mU/L)/405. Hematopoietic cell-specific JNK-deficient mice were generated as described previously (6).

From the [1]Institute of Molecular Biology and Genetics, Seoul National University, Seoul, Korea; the [2]School of Biological Sciences, Seoul National University, Seoul, Korea; the [3]Department of Medicine, Division of Endocrinology and Metabolism, University of California San Diego, La Jolla, California; the [4]Institute of Molecular Cancer Research, University of Zurich, Zurich, Switzerland; and the [5]Department of Biophysics and Chemical Biology, Seoul National University, Seoul, Korea.

Corresponding author: Jae Bum Kim, jaebkim@snu.ac.kr.
Received 15 February 2011 and accepted 13 June 2011.

DOI: 10.2337/db11-0194

This article contains Supplementary Data online at http://diabetes.diabetesjournals.org/lookup/suppl/doi:10.2337/db11-0194/-/DC1.

Y.S.L., P.L., and J.Y.H. contributed equally to this study.

All animal procedures were in accordance with the research guidelines for the use of laboratory animals of Seoul National University and the University of California San Diego.

Flow cytometry analysis. Fluorescence-activated cell sorter analysis (FACS) of stromal vascular cells (SVCs) was performed as described previously (15,16). Epididymal adipose tissue were weighed, rinsed three times in PBS, and then minced in FACS buffer (PBS supplemented with 1% low endotoxin BSA). Tissue suspensions were centrifuged at 500*g* for 5 min and then collagenase-treated (1 mg/mL; Sigma-Aldrich) for 30 min at 37°C with shaking. Cell suspensions were filtered through a 100 μm mesh and centrifuged at 500*g* for 5 min. SVC pellets were then incubated with erythrocyte lysis buffer (ebioscience) for 5 min before centrifuge (300*g*; 5 min) and resuspended in FACS buffer. SVCs were incubated with Fc block for 20 min at 4°C before staining with fluorescence labeled primary antibodies or control IgGs for 30 min at 4°C. F4/80-APC FACS antibody was purchased from AbD Serotec (Raleigh, NC); CD11b-fluorescein isothiocyanate and CD11c-PE FACS antibodies were from BD Biosciences. Cells were gently washed twice and resuspended in FACS buffer with propidium iodide (PI) (Sigma-Aldrich). For Foxp3 staining (ebioscience), SVCs were fixed with Foxp3 staining buffer (ebioscience). After incubation for 5 min at 4°C, cells were washed and then incubated with the fluorescein isothiocyanate-Foxp3 antibody for 30 min at 4°C. SVCs were analyzed using a FACS Aria flow cytometer (BD Biosciences). Unstained, single stains and Fluorescence Minus One controls were used for setting compensation and gates. The events are first gated based on forward versus side scatter area, as well as side scatter height versus width for a total of three dual parameter plots to gate out aggregates and debris. We used single color controls to calculate compensation using the FACSDiva software. A plot of forward scatter versus PI fluorescence was used as the fourth gate to identify individual, live cells. To measure markers with the maximum sensitivity, each fluorochrome was plotted versus PI and polygons were drawn, angled with the aid of the Fluorescence Minus One controls. This excluded dead and autofluorescent cells, but included dim positives. By using polygon gates in combination with logical gates, inclusion of false-positive cells in the gates was reduced.

Glucose uptake assay. Glucose uptake assays were performed as described previously (17).

Macrophage migration assays. Migration of macrophages was measured using Transwell plates (Corning) with a pore size of 8.0 μm. Raw264.7 macrophages were loaded on a top plate. After 3 h, the cells were washed with Dulbecco's modified Eagle's medium supplemented with 0.2% BSA, and the Transwells were transferred to new plates with different adipocyte conditioned media (ACM). Wells were removed, and the cells on the top of the insert or the bottom were scraped and counted by a hematocytometer. The migration rate (%) is the percentage of cells in the bottom versus the total cells in both the bottom and the top. For preparation of ACM, primary adipocytes from lean control or 3-day HFD-treated mice were incubated in Dulbecco's modified Eagle's medium supplemented with 0.2% BSA for 12 h.

Whole-mount immunohistochemistry. Whole-mount immunohistochemistry was performed as described previously (18).

Lipid content measurement. Levels of lipid contents in liver and skeletal muscle of NCD or HFD mice were measured as described previously (19).

Statistics. The results are shown as means ± SEM. All statistical analysis was performed by Student *t* test or ANOVA in Excel (Microsoft); $P < 0.05$ was considered significant.

RESULTS

Effect of short-term HFD on body weight, fat pad mass, and adipocyte size. To determine the temporal transition point when adipose dysfunction begins, C57BL/6J mice were fed a 60% HFD for 3 days and 1, 2, 5, and 10 weeks, and body weight, epididymal adipose tissue mass, and adipocyte size were measured at each time point. At the day of death, all mice were the same age (18 weeks old) in both NCD and HFD groups. Body weight, epididymal adipose tissue mass, and adipocyte size were significantly increased after only 3 days of HFD, and these changes progressed thereafter (Fig. 1). Interestingly, during the first 3 to 4 days of HFD, mice consumed ~30% more food (data not shown) than before or 1 week after HFD regimen, leading to an abrupt increase of body weight during this period, which subsides to a lower rate of increase thereafter. In adipose tissue, the expression of genes involved in lipid storage such as *SREBP1*, *FAS*, *PPAR-γ*, *LXR-α*, and *perilipin* were greatly promoted at 3 days of HFD (Supplementary Fig. 1).

Time course of glucose intolerance and insulin resistance on HFD. To examine whether the increased body weight and adipose tissue mass induced by short-term HFD were associated with systemic insulin resistance, we performed glucose tolerance tests. Mice fed an HFD for only 3 days showed significantly impaired glucose tolerance comparable with that after 10 weeks of HFD (Fig. 2*A*). Plasma insulin levels were also elevated by 3 days of HFD (Fig. 2*B*), further indicating the onset of systemic insulin resistance.

To gain better insight into the in vivo effects of short-term HFD, we performed hyperinsulinemic-euglycemic clamp studies. Basal glucose levels began to rise as early as 3 days of HFD (Fig. 2*C*), and this was accompanied by an increase in basal HGP rates (Fig. 2*D*). These results are consistent with the view that increased basal HGP is the key determinant of basal hyperglycemia. In contrast, the GIR progressively fell, beginning at 3 days with a maximal decrement at 10 weeks of HFD (Fig. 2*E*), demonstrating the onset and progression of systemic insulin resistance. This was accompanied by a gradual decline in ISGDR (Fig. 2*F*) and an impaired ability of insulin to suppress HGP (Fig. 2*G*; Supplementary Fig. 2) and circulating FFA levels (Fig. 2*H*). These in vivo data strongly demonstrate that 3 days of HFD is sufficient to cause decreased insulin sensitivity in muscle, liver, and fat and that the magnitude of the insulin resistance worsens through 10 weeks. It is also evident that the time of onset of insulin resistance and its incremental progression over 10 weeks is comparable in the three major insulin target tissues, liver, muscle, and fat, as indicated by the similar rate of decline in percent HGP suppression, ISGDR, and percent FFA suppression, respectively.

It is well established that adipose tissue dysfunction can contribute to systemic insulin resistance by modulating insulin action in liver and muscle through secreted adipocytokines. To assess this, we measured circulating levels of adiponectin, interleukin (IL)-6, and tumor necrosis factor (TNF)-α. Plasma levels of adiponectin decreased, whereas plasma IL-6 and TNF-α concentrations were increased at 3 days of HFD (Supplementary Fig. 2), without further changes by 10 weeks. These results suggest that rapid dysregulation of adipocytokine production might contribute to the systemic insulin resistance upon short-term HFD.

Effects on adipose tissue inflammation. Adipose tissue inflammation involves increased ATM content with polarization of ATMs into a proinflammatory phenotype, often referred to as M1-like polarization in which ATMs express high levels of CD11c as well as F4/80 and CD11b (3). As shown in Fig. 3*A*, flow cytometry analyses revealed that the total number of F4/80 and CD11b double-positive ATMs were elevated in adipose tissue by 3 days of HFD (*panel* i), and a large proportion of these macrophages also expressed CD11c (triple positive, $F4/80^+$, $CD11b^+$, and $CD11c^+$ proinflammatory M1 ATMs; *panel* ii). This increase in $CD11c^+$ ATM content was also present when data were normalized to total epididymal adipose tissue mass, or total SVC number (%SVCs), showing that proinflammatory macrophages accumulate in adipose tissue shortly after HFD (data not shown). Furthermore, the ratio of $CD11c^+$ ATMs to total ATMs was increased at 3 days of HFD (Fig. 3*A*, *panel* iii). On the other hand, the ratio of $CD11c^-$ ATMs ($F4/80^+$/$CD11b^+$/$CD11c^-$) (%SVCs) was not increased by 3-day HFD (data not shown), although the total number of

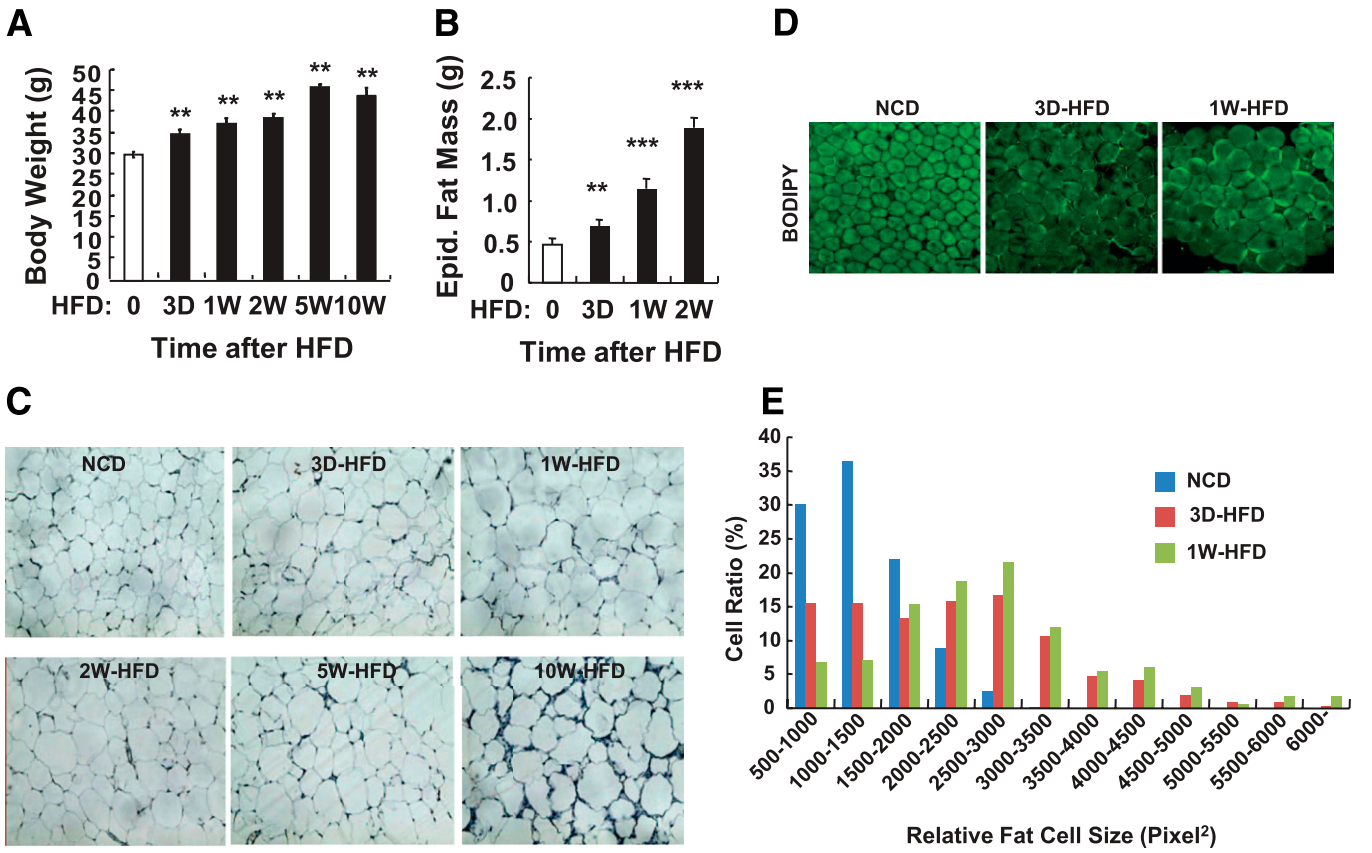

FIG. 1. In 3 days of HFD, body weight, fat mass, and adipocyte size are increased significantly. Eight-week-old C57BL6J male mice were fed NCD until they were subjected to 60% HFD. HFD was treated to the mice 0 (NCD), 3 days (3 D), 1 week (1 W), 2 weeks (2 W), 5 weeks (5 W), or 10 weeks (10 W) before death. At the age of 18 weeks, all mice were killed and subjected to several analyses. *A*: Body weight of the mice at the end of the experiment. $n = 8$ at each time point. Increase of body weight started to be observed by 3 days of HFD. Body weight of mice with 5-week HFD and 10-week HFD was not significantly different. $^{**}P < 0.05$. *B*: Epididymal (Epid.) fat mass. $n = 8$ at each time point. $^{**}P < 0.05$; $^{***}P < 0.001$. *C*: Histology analysis of epididymal adipose tissue. The epididymal adipose tissues were subjected to hematoxylin-eosin staining. $n = 4$ at each time point. *D* and *E*: Further qualitative changes of adipocyte size and morphology by short-term HFD were assessed by histology analysis of whole-mount epididymal adipose tissue. *D*: BODIPY (boron-dipyrromethene) staining of whole-mount adipose tissue from the mice treated with NCD or HFD. Adipocyte size was markedly increased by 3 days of HFD. $n = 6$. Signal intensity of BODIPY staining was adjusted for optimal measurement of adipocyte size using ImageJ software. *E*: Distribution of adipocyte size in epididymal adipose tissue from mice treated with NCD or HFD. (A high-quality digital representation of this figure is available in the online issue.)

$CD11c^-$ ATMs increased (Fig. 3*A*, *panel* iv). Therefore, these results indicate that the proinflammatory M1 polarization of ATMs occurs concomitantly with increased ATM content.

Regulatory T cells (Tregs) are an anti-inflammatory immune cell type and the total number of Tregs was not changed after HFD (Fig. 3*A*, *panel* v). However, the ratio of Tregs to the total number of SVCs (data not shown) or to the total number of $CD11c^+$ macrophages (Fig. 3*A*, *panel* vi) was decreased at 3 days of HFD, remaining equally reduced through 10 weeks. This was because of the increase in ATMs with no absolute change in Treg numbers. Consistent with these FACS data, two-dimensional (paraffin-section; Fig. 3*B*) and three-dimensional (whole-mount; Fig. 3*C*) immunohistochemistry analyses also showed an increase in ATMs by 3 days of HFD.

To determine whether these changes in ATM content during short-term HFD are associated with increased inflammatory gene expression, we assessed mRNA levels of proinflammatory genes by quantitative RT-PCR. As illustrated in Fig. 4 and Supplementary Fig. 3, proinflammatory gene expression was selectively augmented in white adipose tissue after 3 to 7 days of HFD. The increase in proinflammatory gene expression was detected in both the adipocyte and SVC fractions (Supplementary Fig. 3), although the quantitative changes were much greater in the SVCs.

Macrophage chemotaxis. To test whether increased ATM content is associated with increased adipocyte chemoattractant activity, we isolated primary adipocytes from lean control and 3- and 7-day HFD-treated mice and collected ACM from each group. Raw264.7 macrophages were then incubated with ACM in Transwell plates to measure chemotaxis activity. As shown in Fig. 5*A*, macrophage migration was significantly increased with ACM prepared from HFD-treated mice compared with ACM from control chow-fed mice. Consistent with this, monocyte chemoattractant protein (MCP)-1 expression and secretion from primary adipocytes from HFD mice were significantly increased (Fig. 5*B* and *C*). In adipose tissue, interestingly, whereas HFD led to a large increase in *MCP-1* expression in adipocytes, the expression of *MCP-1* in the SVC fraction was unchanged at the end of the 7-day HFD period (Supplementary Fig. 3). In contrast, *TNF-α* and *IL-6* expression was predominantly from SVCs, not adipocytes (Supplementary Fig. 3). These data indicate that enhanced macrophage infiltration into adipose tissue after short-term HFD is a result of increased adipocyte-derived chemoattractive activity.

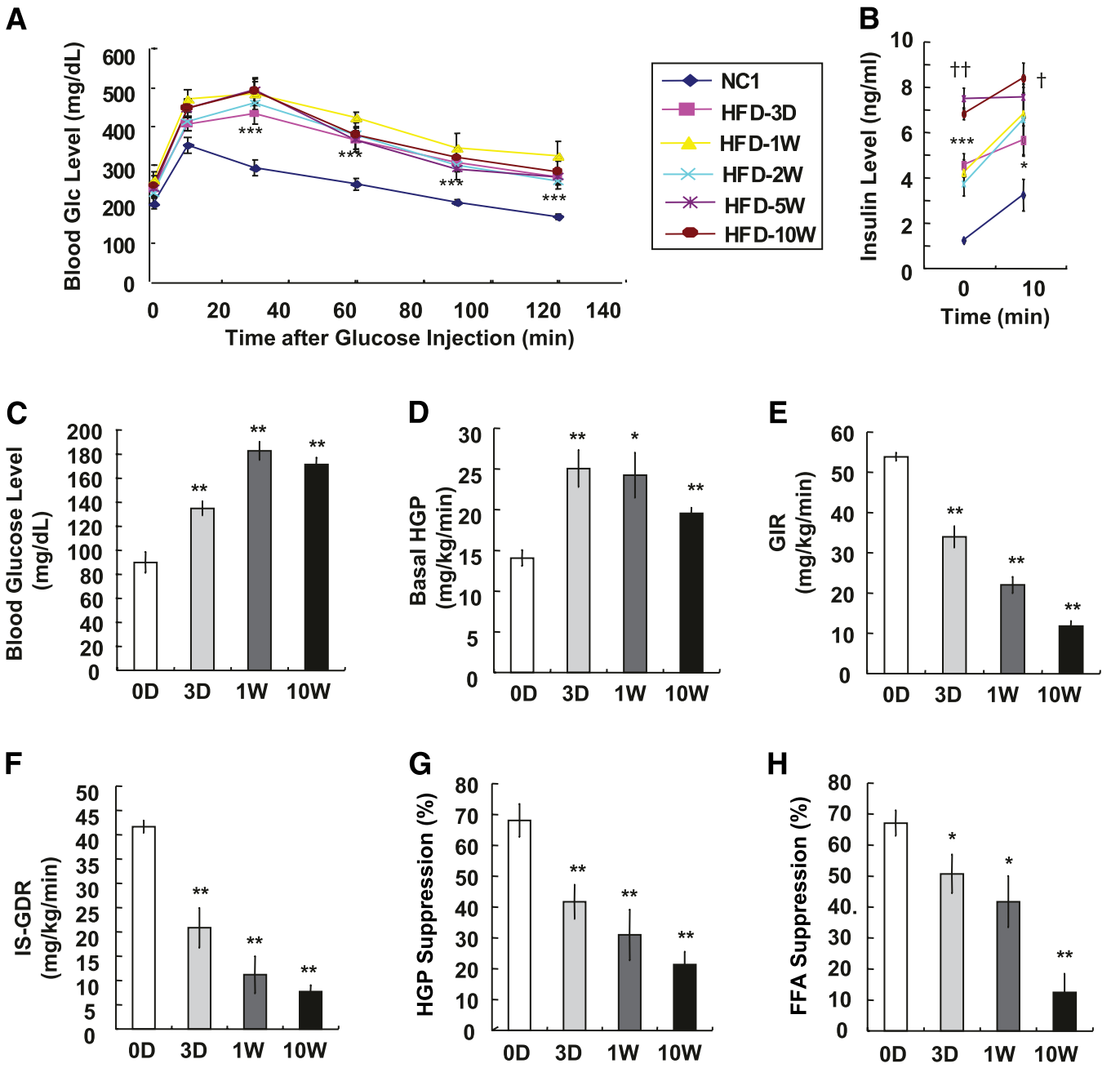

FIG. 2. HFD induces systemic insulin resistance in 3 days. ***A*: C57BL/6J male mice were treated with NCD or HFD and subjected to oral glucose (Glc) tolerance test. $n = 8$ at each time point. ***$P < 0.001$ NCD vs. 3-day HFD. *B*: Blood insulin levels at time 0 and 10 min after glucose injection. Basal insulin level was significantly elevated by 3 days of HFD and then further increase was detected significantly by 5 and 10 weeks of HFD. $n = 8$. *$P < 0.05$ NCD vs. 3-day HFD; ***$P < 0.001$ NCD vs. 3-day HFD; †$P < 0.05$ 3-day HFD vs. 10-week HFD; ††$P < 0.01$ 3-day HFD vs. 10-week HFD. *C–H*: Hyperinsulinemic-euglycemic clamp was performed in mice treated with HFD for different periods; $n = 8$ (NCD, and 3-day and 1-week HFD mice) or $n = 6$ (10-week HFD mice). *C*: Basal blood glucose level (before clamp). **$P < 0.01$. *D*: Basal hepatic glucose production. *$P < 0.05$; **$P < 0.01$. *E*: GIR. **$P < 0.01$. *F*: ISGDR. **$P < 0.01$. *G*: Insulin-dependent suppression of hepatic glucose. **$P < 0.01$. *H*: Suppression of plasma FFA level by insulin. *$P < 0.05$; **$P < 0.01$.**

Lymphocytes are not necessary for short-term HFD-induced insulin resistance. To examine the potential role of lymphocytes in the systemic insulin resistance and adipose tissue inflammation induced by short-term HFD, we used lymphocyte-deficient Rag1 KO mice. Consistent with previous reports (20), NCD-fed Rag1 KO mice showed higher levels of basal ATM infiltration and M1 polarization than those of wild-type mice (Fig. 6*A*). After 1 week of HFD, a significant increase in ATM infiltration and M1 polarization was observed in Rag1 KO mice along with increased fat mass and inflammatory gene expression (Fig. 6*A–C*). Additionally, Rag1 KO mice developed glucose intolerance as early as 3 days of HFD with increased blood insulin levels (Fig. 6*D* and *E*). Moreover, insulin tolerance tests indicated that Rag1 KO mice exhibited a similar level of insulin resistance as wild-type mice by 1-week HFD (Fig. 6*F*). In vitro glucose uptake assays showed that primary adipocytes from 1-week HFD-fed Rag1 KO mice were insulin resistant (Fig. 6*G*). Together, these results suggest that lymphocytes are not necessary for short-term HFD-induced adipose dysfunction and insulin resistance.

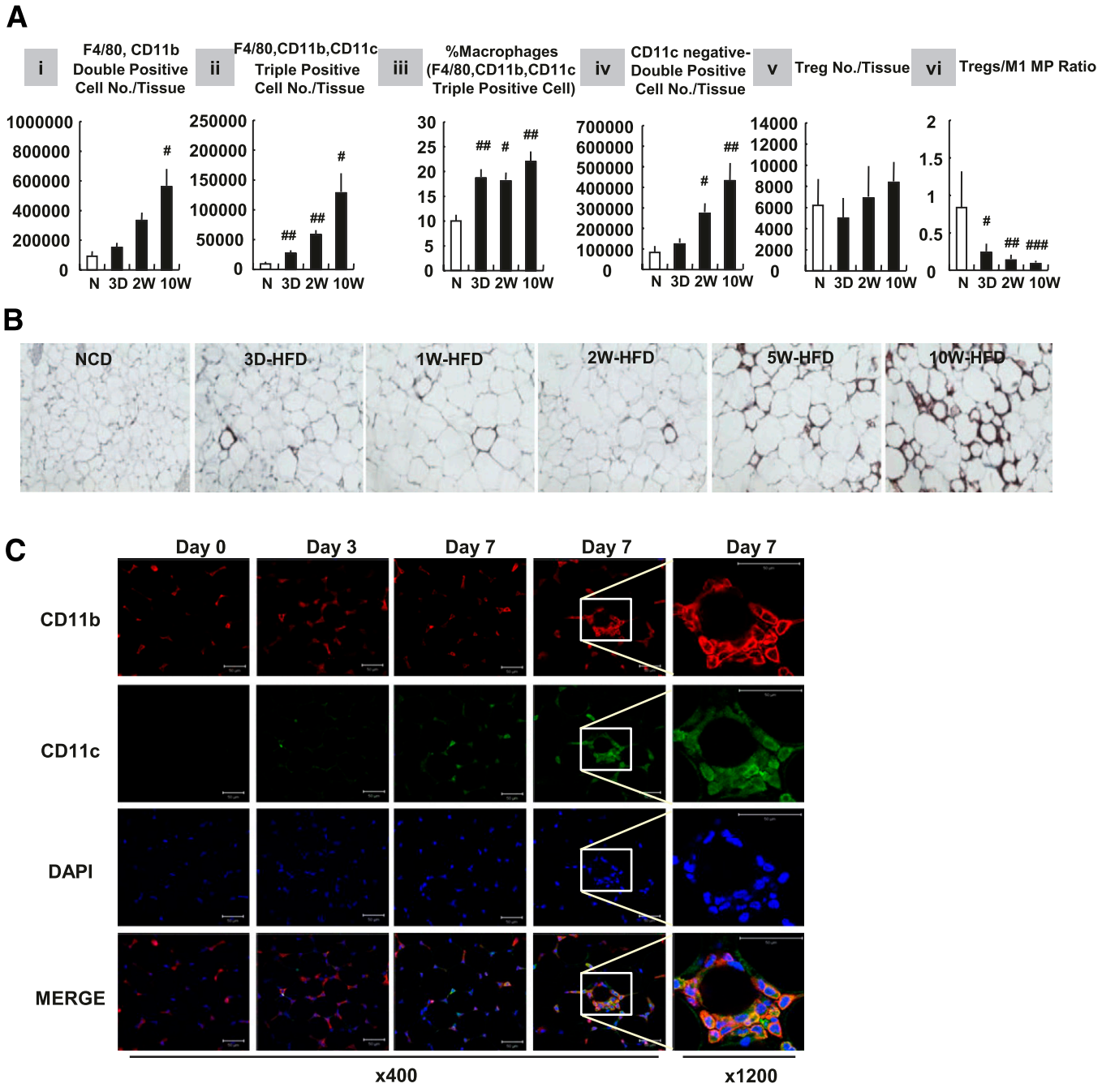

FIG. 3. Macrophage (MP) infiltration and polarization increase in 3 days of HFD. Mice were treated with NCD (N) or HFD for a series of periods as indicated: 3D, 3 days; 2W, 2 weeks; 10W, 10 weeks. After 10 weeks from when first mice were fed an HFD, mice were killed and epididymal adipose tissues were taken for further analyses. *A*: Flow cytometry analyses of immune cells in stromal vascular fraction of adipose tissue. #$P < 0.05$; ##$P < 0.01$; ###$P < 0.001$; $n = 4$ (NCD and 2-week HFD mice) or $n = 6$ (1-week and 10-week HFD mice). *B*: Immunohistochemistry analysis of epididymal adipose tissue. The epididymal adipose tissues were stained with antibodies against MAC2 and then subjected to hematoxylin-eosin staining. $n = 4$. *C*: Whole-mount immunohistochemistry analysis of epididymal adipose tissue from NCD or 3- or 7-day HFD-treated mice. Samples were stained with DAPI (blue) or antibodies against CD11b (red) and CD11c (green) and visualized by multiphoton confocal microscopy. Scale bar denotes 50 μm. (A high-quality digital representation of this figure is available in the online issue.)

Macrophages are not critical for short-term HFD-induced insulin resistance. To determine whether macrophages are essential for the initiation of HFD-induced insulin resistance, we tested the effect of clodronate-mediated depletion of macrophages on insulin sensitivity in 3-day HFD-fed mice. After clodronate injection (48 h), ATMs were depleted by 80%, and this effect was sustained for up to 3 days (Fig. 7*A*). Under the same conditions, there were no detectable changes in adipocyte size or morphology (Fig. 7*B*). Despite that, serum levels of pro-inflammatory cytokines such as IL-6 and TNF-α were significantly decreased by clodronate (Fig. 7*C*). Interestingly, glucose uptake assays in primary adipocytes revealed that clodronate-mediated depletion of macrophages did not restore the HFD-induced decrease in insulin-stimulated glucose uptake (Fig. 7*D*). Moreover, clodronate treatment did not improve glucose tolerance or insulin resistance in mice fed an HFD for 3 or 7 days (Fig. 7*E–G*). Because clodronate

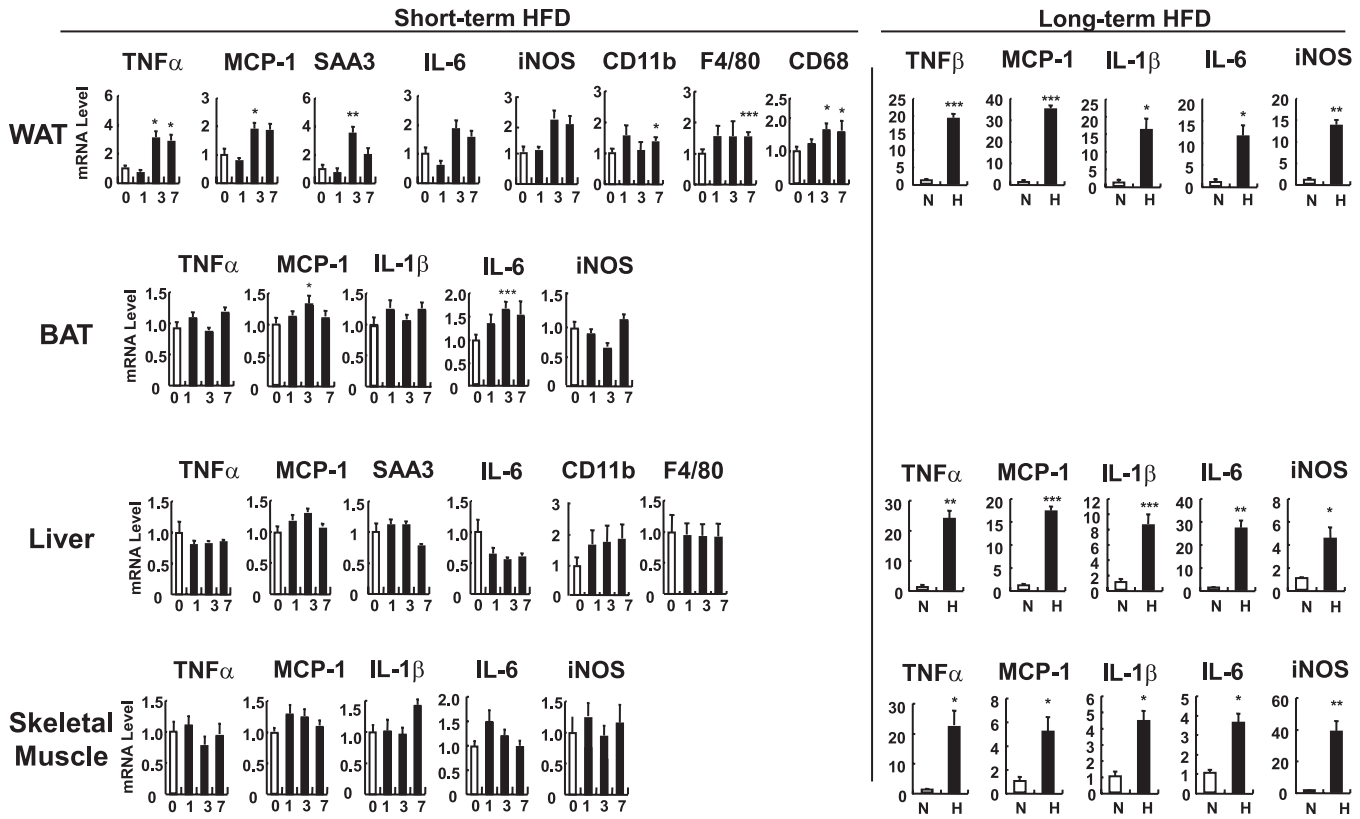

FIG. 4. Inflammatory gene expression is induced in 3 days after HFD. C57BL/6J mice were treated with an HFD. Mice were fed an HFD for 0 (0 or N [NCD]), 1 (1), 3 (3), or 7 days (7), or 16 weeks (H). mRNA levels of inflammatory genes from epididymal adipose tissue (WAT), brown adipose tissue (BAT), liver, and skeletal muscle were measured by quantitative real-time RT-PCR analysis. $n = 10$ at each time point. *$P < 0.05$; **$P < 0.01$; ***$P < 0.001$. iNOS, inducible nitric oxide synthase; SAA3, serum amyloid A3.

targets all phagocytic cell populations, including hepatic Kupffer cells (Supplementary Fig. 4), we also tested the Kupffer cell inhibitor, gadolinium. Similar to clodronate, gadolinium did not affect 1-week HFD-induced glucose intolerance (Supplementary Fig. 5). In marked contrast, both clodronate and gadolinium significantly improved glucose tolerance in long-term (14-week) HFD-treated mice (Supplementary Fig. 6) or obese/diabetic *db/db* mice (data not shown). These results are consistent with our previous report that depletion of proinflammatory macrophages readily reverses the insulin resistance in well-established obesity (7). Thus, these data suggest that ATMs and Kupffer cells do not play a critical role in the insulin resistance caused by short-term HFD but are essential for the development of insulin resistance after long-term (14-week) HFD.

To assess this concept with an alternative approach, we determined the effect of suppressing proinflammatory activity in immune cells using hematopoietic cell-specific JNK-deficient mice. Previously, we have shown that hematopoietic cell-specific JNK deficiency protects mice from long-term HFD-induced insulin resistance (6). As shown in Fig. 7*H*–*J*, hematopoietic cell-specific JNK deficiency did not ameliorate short-term HFD-induced insulin resistance. These results are consistent with the idea that macrophage-mediated inflammation is necessary for the insulin resistance associated with long-term HFD/obesity, but not as a result of short-term HFD.

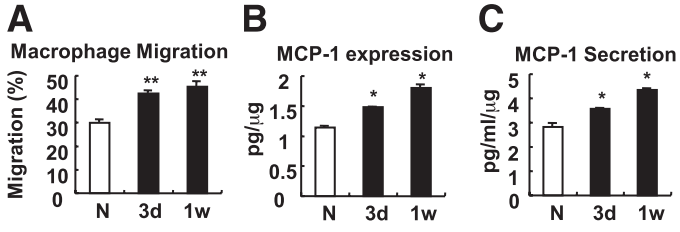

FIG. 5. Adipocytes become more chemoattractive to macrophages after 3 days of HFD. *A*: Macrophage migration assays using primary ACM from mice treated with NCD (N) or HFD. ACM were obtained by incubating mouse primary adipocytes in serum-free Dulbecco's modified Eagle's medium for 12 h. 3d, 3 days; 1w, 1 week. *B*: MCP-1 protein expression from the primary adipocytes. *C*: MCP-1 protein secretion from those adipocytes. *$P < 0.05$; **$P < 0.01$.

Ceramide accumulates in liver and muscle acutely after HFD. A number of studies have shown that insulin resistance in obesity is associated with activation of intracellular diacylglycerol (DAG)/protein kinase C (PKC)θ and ceramide pathways (10,21). To determine whether lipid overload as a result of short-term HFD is associated with systemic insulin resistance, we measured various lipid components in liver and skeletal muscle of NCD mice after 3 days of HFD. As shown in Fig. 8, levels of triacylglycerol, nonesterified fatty acids (NEFA), DAG, and ceramide were all significantly increased in liver and skeletal muscle by 3 days of HFD. Of interest, clodronate treatment did not affect short-term HFD-induced accumulation of DAG, ceramide, and NEFA in liver and skeletal muscle, whereas it blunted triacylglycerol content (Fig. 8).

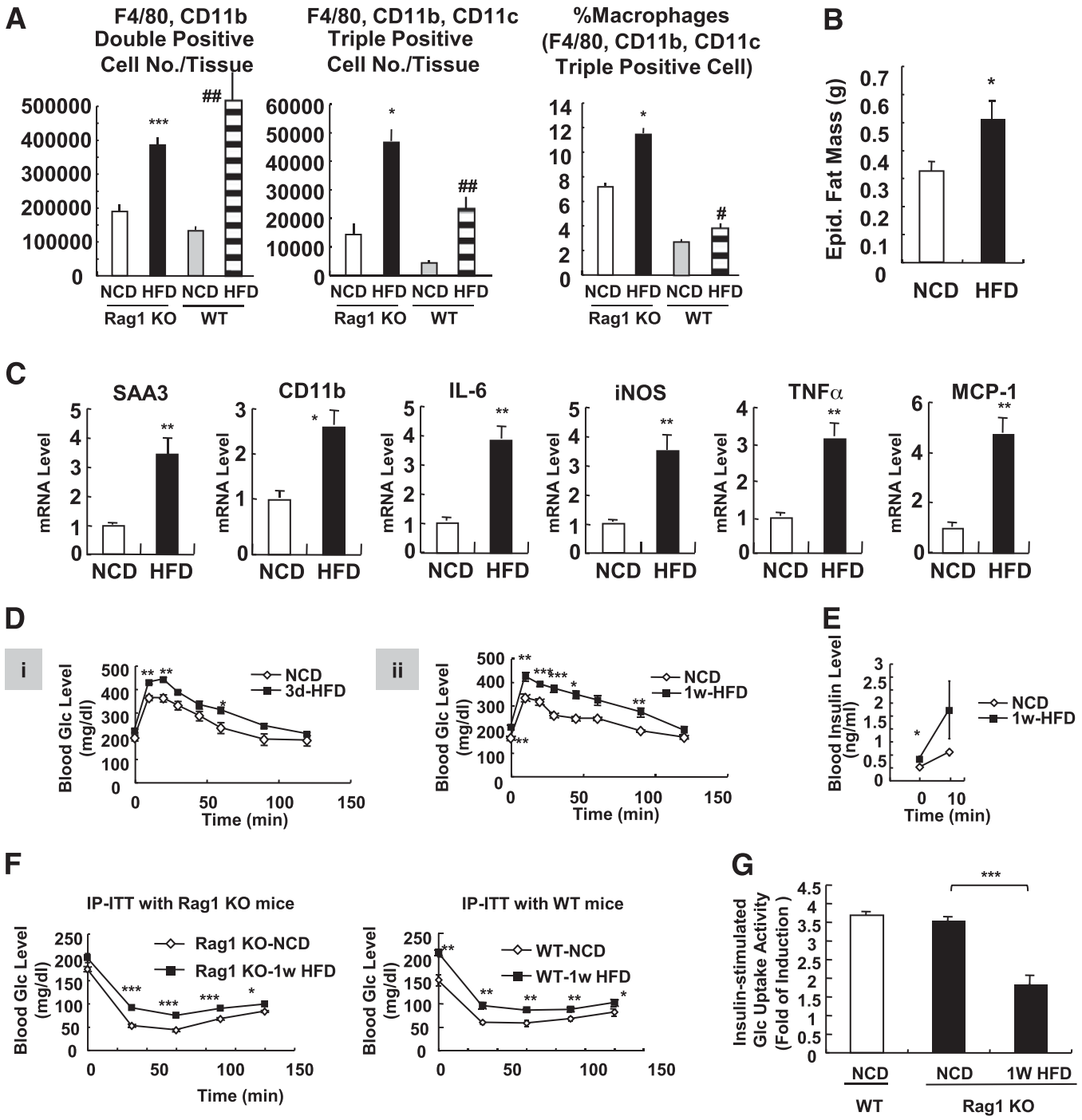

FIG. 6. Rag1 KO mice develop insulin resistance with increased macrophage activation in 1 week of HFD. *A*: Macrophage infiltration and M1 polarization were increased by short-term HFD. Rag1 KO mice were treated with HFD for 1 week and killed, and epididymal adipose tissues were taken for further analyses. Total macrophages (double positive; F4/80$^+$, CD11b$^+$) and CD11c$^+$ macrophages (triple positive cells; F4/80$^+$, CD11b$^+$, CD11c$^+$) were increased in adipose tissue in 1 week of HFD. *P < 0.05 KO-NCD vs. KO HFD; ***P < 0.001 KO-NCD vs. KO HFD; #P < 0.05 wild-type (WT)-NCD vs. WT HFD; ##P < 0.01 WT-NCD vs. WT HFD. n = 6. *B*: Epididymal (Epid.) adipose tissue mass in NCD and 1-week HFD-treated Rag1 KO mice. *C*: Expression of inflammatory genes was promoted in 1-week HFD-fed Rag1 KO mice. mRNA levels of inflammatory genes from epididymal adipose tissue were measured by quantitative real-time RT-PCR analysis. *D–F*: HFD rapidly induces systemic insulin resistance in Rag1 KO mice. *D*: Rag1 KO mice (8 weeks old, male) were treated with NCD or HFD for 3 days (3d) (i) or 1 week (1w) (ii) and subjected to oral glucose (Glc) tolerance test. *E*: Serum insulin levels of Rag1 KO mice treated with NCD or HFD (for 1 week) during oral glucose tolerance. 0 min, before glucose injection; 10 min, 10 min after glucose injection. *F*: WT or Rag1 KO mice were treated with NCD or HFD for 1 week and subjected to insulin tolerance test with intraperitoneal injection of insulin (IP-ITT). Blood glucose levels were measured at 0, 30, 60, 90, and 120 min after insulin (0.4 unit/kg) injection. *G*: Glucose-uptake assays using primary adipocytes from mice treated with NCD or HFD for 1 week. iNOS, inducible nitric oxide synthase; SAA3, serum amyloid A3. *P < 0.05; **P < 0.01; ***P < 0.001.

DISCUSSION

Here, we have evaluated the in vitro and in vivo initiation and progression of inflammation and insulin resistance during the development of obesity in HFD-fed mice. Because of the temporal nature of this study, we were able to assess the causes of insulin resistance in the early stages of HFD-induced obesity, as well as later on in this process after obesity was well established. We found that glucose

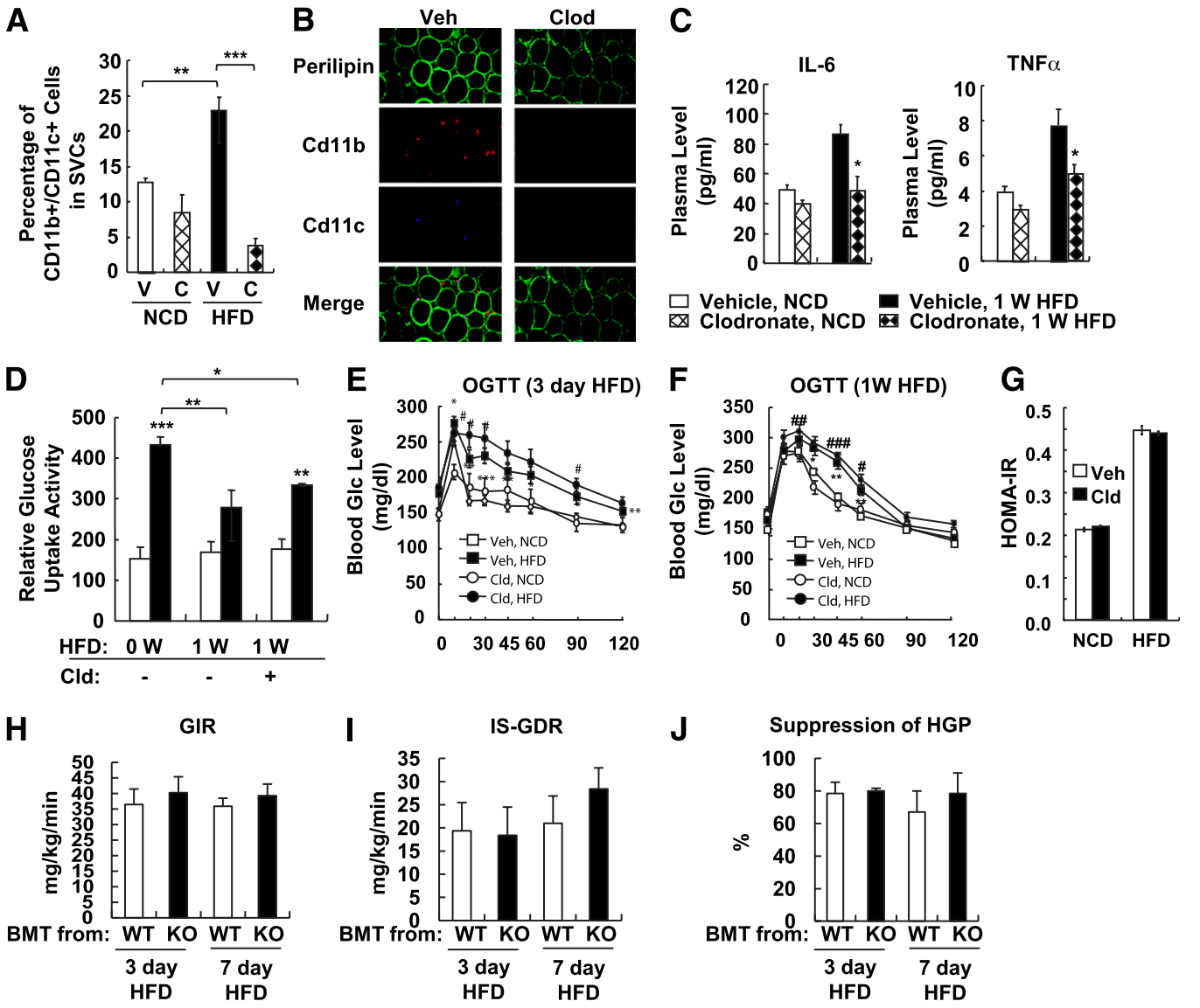

FIG. 7. Macrophage depletion using clodronate-liposomes does not affect short-term HFD-dependent adipocyte insulin resistance. Mice were treated with NCD or 60% HFD in the presence or absence of clodronate injection. Mice were given clodronate injection (100 mg/kg i.p.) 3 days before HFD, which was followed by a second and third injection every 3 days (at days 0 and 3). *A*: Flow cytometry analysis of CD11c$^+$ macrophages in adipose tissue. V, vehicle (empty liposomes); C, clodronate-liposomes. *B*: Whole-mount immunohistochemistry analysis of epididymal adipose tissue. Veh, vehicle; Clod, clodronate-liposomes. *C*: Cytokine concentration in the mouse sera injected with vehicle and clodronate. W, week. *$P < 0.05$. *D*: Glucose-uptake assays using primary adipocytes from mice treated with NCD or HFD for 1 week with or without clodronate injection. White columns denote relative glucose uptake activity without insulin. Black columns denote relative glucose uptake activity with insulin. Cld, clodronate-liposomes. *E*: Oral glucose tolerance test (OGTT) of mice treated with HFD for 3 days. #$P < 0.05$ Veh-NCD vs. Veh-HFD; *$P < 0.05$ Cld-NCD vs. Cld-HFD; **$P < 0.01$ Cld-NCD vs. Cld-HFD; ***$P < 0.001$ Cld-NCD vs. Cld-HFD. $n = 6$. *F*: Glucose tolerance test of mice treated with HFD for 7 days. #$P < 0.05$ Veh-NCD vs. Veh-HFD; ##$P < 0.01$ Veh-NCD vs. Veh-HFD; ###$P < 0.001$ Veh-NCD vs. Veh-HFD; *$P < 0.05$ Cld-NCD vs. Cld-HFD; **$P < 0.01$ Cld-NCD vs. Cld-HFD. $n = 6$. *G*: Homeostasis model assessment of insulin resistance (HOMA-IR). *H–J*: Hematopoietic cell-specific JNK deficiency does not affect short-term HFD-induced insulin resistance. For the generation of radiation chimera, C57BL/6J mice received a lethal dose of 10 Gy of ionizing radiation, followed by tail vein injection of 10^7 bone marrow cells either from wild-type (WT) or JNK KO mice. After 6 weeks of bone marrow reconstitution, mice were subjected to 3 or 7 days of HFD, followed by hyperinsulinemic-euglycemic clamp. $n = 4$ to 5. *H*: GIR. *I*: ISGDR. *J*: Insulin-dependent hepatic glucose suppression. BMT, bone marrow transplantation. (A high-quality digital representation of this figure is available in the online issue.)

intolerance and systemic insulin resistance developed by 3 days of HFD. The systemic insulin resistance steadily worsened with increasing adipose tissue inflammation, and the temporal sequence and magnitude of initiation and progression of decreased insulin sensitivity was comparable in muscle, adipose tissue, and liver. Concurrently, a variety of markers of inflammation can be readily detected in adipose tissue, by as early as 3 days, and progressively increased throughout the 10-week HFD-feeding period. However, in liver and skeletal muscle, increased inflammation became apparent only after several weeks into the HFD period, after obesity was well established (Fig. 4). Furthermore, depletion of macrophages or Kupffer cells by clodronate-liposomes or gadolinium administration or disruption of macrophage inflammatory pathways by JNK1 deletion did not attenuate the early stage of insulin resistance (Fig. 7 and Supplementary Fig. 5). In contrast, these maneuvers substantially ameliorated insulin resistance at 14 weeks of HFD, at a time when severe obesity was established (Supplementary Fig. 6). Thus, our data suggest that macrophage-mediated tissue inflammation is a key component of chronic obesity–associated insulin

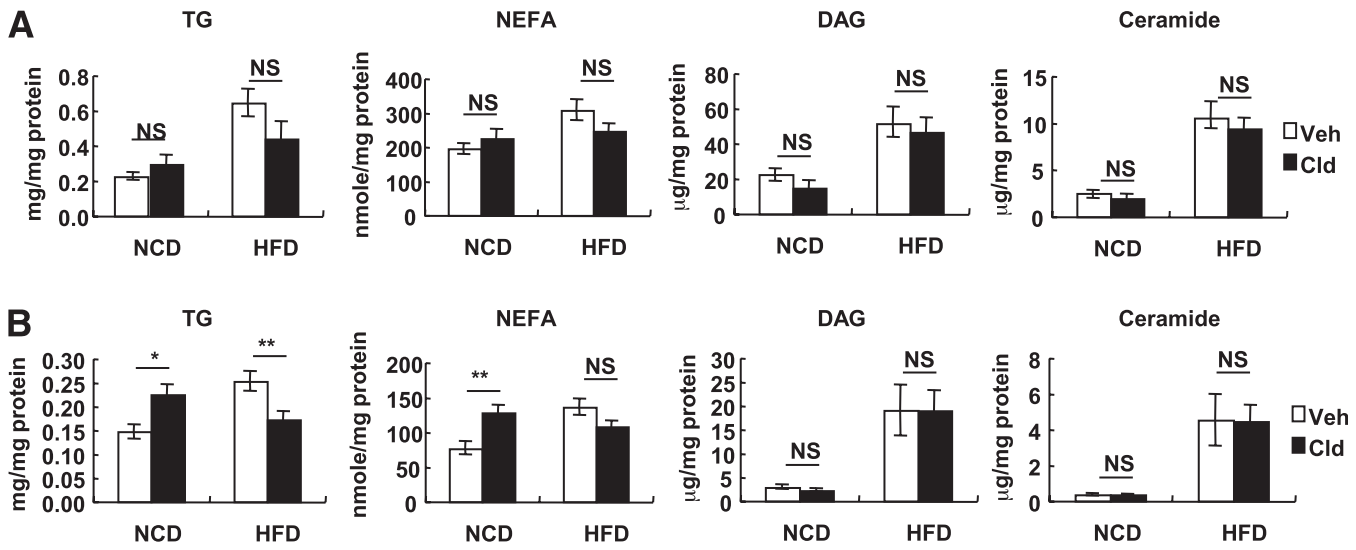

FIG. 8. Lipid contents of liver and skeletal muscle after 3 days of HFD. Eighteen-week-old C57BL6J male chow-fed mice were started in 60% HFD at day 0 for 3 days before the analyses. A separate group of age-matched chow-fed mice was studied as controls. For the macrophage depletion experiment, two shots of clodronate injection (100 mg/kg i.p.) were given at day −3 and 0. Veh, vehicle; Clod, clodronate-liposomes; TG, triacylglyceride; NS, not significant. *A*: Lipid contents in liver. *B*: Lipid contents in skeletal muscle. $n = 8$. *$P < 0.05$; **$P < 0.01$.

resistance but is not critical for the decrease in insulin sensitivity, which develops at the early stage of HFD feeding.

Our data indicate that the inflammation elicited by short-term HFD was not sufficient to induce insulin resistance. Although elevation of inflammatory gene expression in adipose tissue and macrophage infiltration were significant at 3 days of HFD, the fold of increase by 3 or 7 days of HFD was much lower than that observed by 16 weeks of HFD (Fig. 4). Moreover, inflammation in muscle and liver was not observed during short-term HFD, in contrast with long-term 16-week HFD, suggesting that inflammation initiated in adipose tissue by short-term HFD was not able to propagate to other tissues as to induce insulin resistance.

Within the first several days of HFD, changes in circulating adipocytokine concentrations were observed (decreased adiponectin, increased TNF-α, and IL-6), which could contribute to decreased systemic insulin sensitivity, suggesting that acute induction of adipose tissue dysfunction might play important roles in short-term HFD-induced systemic insulin resistance. However, it is interesting to note that although insulin resistance progressively worsened from 3 days to 10 weeks, no further changes in adipocytokine levels were detected, indicating that some other mechanism must be responsible for the steady progression of the degree of insulin resistance. The chronic tissue inflammatory state is an excellent candidate for this mechanism, since accumulation of proinflammatory macrophages in adipose tissue gradually increased throughout the 10-week study period, and the increase in ATMs correlated very well with the magnitude of the insulin resistance (Fig. 4). Furthermore, increased inflammation in muscle and liver was only detected in the later stages of HFD, as systemic insulin resistance worsened. Thus, chronic tissue inflammation is at least one major cause of systemic insulin resistance associated with the obese state.

A possible mechanism for the early phase of insulin resistance seems to also relate to the lipid overload observed at the onset of HFD. It has been shown that intravenous lipid infusions rapidly cause systemic insulin resistance in humans and mice (9,11,21–25) and that this can be blunted by genetic ablation of PKCθ (10). This is associated with increased cellular levels of DAGs, ceramides, and other lipid-derived molecules, and this process of lipid-induced insulin resistance is termed lipotoxicity. Indeed, we observed that ceramide, DAG, and NEFA levels were increased in muscle and liver by 3 days of HFD and were not affected by clodronate treatment (Fig. 8). Thus, it seems possible that the large excess lipid intake at the onset of HFD would trigger decreased insulin sensitivity through an acute lipotoxic mechanism, whereas chronic tissue inflammation emerges as a key cause of insulin resistance during the established stage of obesity. It is of interest that the timing of the onset and the progressive worsening of the insulin resistance is comparable across the three major insulin target tissues, muscle, liver, and fat, despite the fact that the underlying mechanisms evolve during transition from the early to the later stages of HFD feeding and development of obesity.

Glucose intolerance, as well as increased HGP, was observed by 3 days of HFD and did not worsen throughout the next 10 weeks; i.e., these changes were nonprogressive. In contrast, although insulin resistance was readily detected by 3 days of HFD, it was progressively more severe by 1 week and then even more so by 10 weeks. This raises the question as to why glucose intolerance does not worsen with the progression of insulin resistance. A likely reason relates to the circulating insulin levels. Insulin levels are substantially higher at the later stages of HFD, compared with the earlier time points (Fig. 2*B*). This indicates that progressive hyperinsulinemia, most likely as a result of increasing β-cell hyperplasia (data not shown), increases over the later stages of HFD, compensating for the worsening insulin resistance state. However, this compensation does not reregulate glucose tolerance to normal but maintains glucose tolerance at the same level as observed during the initial 3-day HFD time point.

Recently, it has been found that adipose inflammation and increased ATM infiltration in obesity is accompanied by changes in subpopulations of T cells such as Tregs and $CD8^+$ T cells residing in adipose tissue (26,27). We observed that the total number of Tregs in the epididymal adipose tissue was not decreased at any point during the

10-week HFD period, whereas the ratio of Tregs to the other cell types in SVCs, especially to M1-like macrophages, decreased significantly (Fig. 3*A*). These results are consistent with the view that passive changes in Treg ratios in adipose tissue, but not active suppression of Treg infiltration or proliferation, can be correlated with adipose tissue remodeling and ATM accumulation, conferring adipose tissue inflammation. Although this relative change in Treg proportions might contribute to migration or activation of ATMs, the macrophages would likely still be the effector cells promoting decreased insulin sensitivity in obesity. Moreover, lymphocyte-deficient Rag1 KO mice were not protected from short-term HFD-induced insulin resistance and glucose intolerance, or ATM accumulation (Fig. 6). Therefore it is likely that lymphocytes do not significantly contribute to short-term HFD-induced insulin resistance and adipose tissue inflammation.

In summary, we have assessed the temporal events underlying the development of insulin resistance during high-fat feeding. We found that decreased systemic insulin sensitivity appears early in the course of HFD and progressively increases at similar rates in muscle, liver, and adipose tissue. Interestingly, different mechanisms appear to evolve over the 10-week HFD period; i.e., lipid overload and lipotoxicity are more important early on, whereas chronic inflammation emerges as a more dominant mechanism once obesity is established toward the end of the HFD period.

ACKNOWLEDGMENTS

This work was supported by grants from the Korea Science and Engineering Foundation funded by the Korean government (Ministry of Education, Science and Technology; SC-3230, 2009-0091913, 20110018312, and R312009000100320); by the National Institutes of Health (NIH) grants DK-033651, DK-074868, T32-DK-007494, and DK-063491; and by the Eunice Kennedy Shriver National Institute of Child Health and Human Development/NIH through cooperative agreement of U54-HD-012303-25 as part of the specialized Cooperative Centers Program in Reproduction and Infertility Research. J.Y.H., I.J.H., and J.I.K. were supported by a BK21 Research Fellowship from the Ministry of Education and Human Resources Development.

No potential conflicts of interest relevant to this article were reported.

Y.S.L. wrote the manuscript and researched data. P.L., J.Y.H., I.J.H., M.L., J.I.K., M.H., S.T., A.C., W.J.L., and G.K.B. researched data. R.S. researched data and reviewed and edited the manuscript. J.O. and J.B.K. contributed to discussion and reviewed and edited the manuscript.

REFERENCES

1. Weisberg SP, McCann D, Desai M, Rosenbaum M, Leibel RL, Ferrante AW Jr. Obesity is associated with macrophage accumulation in adipose tissue. J Clin Invest 2003;112:1796–1808
2. Xu H, Barnes GT, Yang Q, et al. Chronic inflammation in fat plays a crucial role in the development of obesity-related insulin resistance. J Clin Invest 2003;112:1821–1830
3. Nguyen MT, Favelyukis S, Nguyen AK, et al. A subpopulation of macrophages infiltrates hypertrophic adipose tissue and is activated by free fatty acids via toll-like receptors 2 and 4 and JNK-dependent pathways. J Biol Chem 2007;282:35279–35292
4. Lumeng CN, Bodzin JL, Saltiel AR. Obesity induces a phenotypic switch in adipose tissue macrophage polarization. J Clin Invest 2007;117:175–184
5. Lumeng CN, DelProposto JB, Westcott DJ, Saltiel AR. Phenotypic switching of adipose tissue macrophages with obesity is generated by spatiotemporal differences in macrophage subtypes. Diabetes 2008;57:3239–3246
6. Solinas G, Vilcu C, Neels JG, et al. JNK1 in hematopoietically derived cells contributes to diet-induced inflammation and insulin resistance without affecting obesity. Cell Metab 2007;6:386–397
7. Patsouris D, Li PP, Thapar D, Chapman J, Olefsky JM, Neels JG. Ablation of CD11c-positive cells normalizes insulin sensitivity in obese insulin resistant animals. Cell Metab 2008;8:301–309
8. Saberi M, Woods NB, de Luca C, et al. Hematopoietic cell-specific deletion of toll-like receptor 4 ameliorates hepatic and adipose tissue insulin resistance in high-fat-fed mice. Cell Metab 2009;10:419–429
9. Kim JK, Kim YJ, Fillmore JJ, et al. Prevention of fat-induced insulin resistance by salicylate. J Clin Invest 2001;108:437–446
10. Kim JK, Fillmore JJ, Sunshine MJ, et al. PKC-theta knockout mice are protected from fat-induced insulin resistance. J Clin Invest 2004;114:823–827
11. Shi H, Kokoeva MV, Inouye K, Tzameli I, Yin H, Flier JS. TLR4 links innate immunity and fatty acid-induced insulin resistance. J Clin Invest 2006;116:3015–3025
12. Kolditz CI, Langin D. Adipose tissue lipolysis. Curr Opin Clin Nutr Metab Care 2010;13:377–381
13. Hevener AL, He W, Barak Y, et al. Muscle-specific Pparg deletion causes insulin resistance. Nat Med 2003;9:1491–1497
14. Zeisberger SM, Odermatt B, Marty C, Zehnder-Fjällman AH, Ballmer-Hofer K, Schwendener RA. Clodronate-liposome-mediated depletion of tumour-associated macrophages: a new and highly effective antiangiogenic therapy approach. Br J Cancer 2006;95:272–281
15. Li P, Lu M, Nguyen MT, et al. Functional heterogeneity of CD11c-positive adipose tissue macrophages in diet-induced obese mice. J Biol Chem 2010;285:15333–15345
16. Oh DY, Talukdar S, Bae EJ, et al. GPR120 is an omega-3 fatty acid receptor mediating potent anti-inflammatory and insulin-sensitizing effects. Cell 2010;142:687–698
17. Lee YS, Kim AY, Choi JW, et al. Dysregulation of adipose glutathione peroxidase 3 in obesity contributes to local and systemic oxidative stress. Mol Endocrinol 2008;22:2176–2189
18. Lee YS, Choi JW, Hwang I, et al. Adipocytokine orosomucoid integrates inflammatory and metabolic signals to preserve energy homeostasis by resolving immoderate inflammation. J Biol Chem 2010;285:22174–22185
19. Bandyopadhyay GK, Lee LY, Guzman RC, Nandi S. Effect of reproductive states on lipid mobilization and linoleic acid metabolism in mammary glands. Lipids 1995;30:155–162
20. Winer S, Chan Y, Paltser G, et al. Normalization of obesity-associated insulin resistance through immunotherapy. Nat Med 2009;15:921–929
21. Holland WL, Brozinick JT, Wang LP, et al. Inhibition of ceramide synthesis ameliorates glucocorticoid-, saturated-fat-, and obesity-induced insulin resistance. Cell Metab 2007;5:167–179
22. Frangioudakis G, Cooney GJ. Acute elevation of circulating fatty acids impairs downstream insulin signalling in rat skeletal muscle in vivo independent of effects on stress signalling. J Endocrinol 2008;197:277–285
23. Roden M, Price TB, Perseghin G, et al. Mechanism of free fatty acid-induced insulin resistance in humans. J Clin Invest 1996;97:2859–2865
24. Ferrannini E, Barrett EJ, Bevilacqua S, DeFronzo RA. Effect of fatty acids on glucose production and utilization in man. J Clin Invest 1983;72:1737–1747
25. Randle PJ, Newsholme EA, Garland PB. Regulation of glucose uptake by muscle. 8. Effects of fatty acids, ketone bodies and pyruvate, and of alloxan-diabetes and starvation, on the uptake and metabolic fate of glucose in rat heart and diaphragm muscles. Biochem J 1964;93:652–665
26. Feuerer M, Herrero L, Cipolletta D, et al. Lean, but not obese, fat is enriched for a unique population of regulatory T cells that affect metabolic parameters. Nat Med 2009;15:930–939
27. Nishimura S, Manabe I, Nagasaki M, et al. CD8+ effector T cells contribute to macrophage recruitment and adipose tissue inflammation in obesity. Nat Med 2009;15:914–920